2014 International Conference on Unmanned Aircraft Systems (ICUAS)
May 27-30, 2014. Orlando, FL, USA

Survey on Attitude and Heading Reference Systems for Remotely Piloted Aircraft Systems

Miguel Cordero, Francisco Alarcón, Antonio Jiménez, Antidio Viguria and Aníbal Ollero

Abstract— **Attitude estimation is a critical task for the safe navigation of RPAS (Remotely Piloted Aircraft System). When no 3D positioning information is available, e.g. due to GNSS (Global Navigation Satellite System) blockage, the autopilot must use data from the rest of the onboard navigation sensors to fly the RPAS in a stable manner and reduce potential damage on the ground. Hence, using accurate and efficient Attitude and Heading Reference System (AHRS) algorithms is of vital importance for the safety of the system. Different AHRS algorithms based on Kalman Filtering (KF) or Extended Kalman Filtering (EKF) have been proposed in the literature but there are only few works comparing them using experimental data collected with real sensors. In this paper three different AHRS algorithms have been compared using real sensor data collected with a commercial system (Xsens MTi-G). Additionally, one of these algorithms has been implemented in two autopilot platforms developed by CATEC and their performances have been compared with the Xsens MTi-G system. For assessing the accuracy of AHRS systems, the attitude estimations provided by the system needs to be compared with the attitude values that are considered to be a ground truth. In this paper, a multi-camera based motion capture system from VICON Motion System Ltd has been used to obtain the attitude ground truth. This system can estimate the position of each marker with sub-millimetric accuracy and the attitude of the object with an accuracy of less than a tenth of a degree.**

I. INTRODUCTION

In normal operation, RPAS (Remotely Piloted Aircraft Systems) use attitude, position and velocity information estimated from data provided by the navigation sensors onboard to follow a given path of waypoints. Three-dimension positioning and velocity are estimated using an INS/GNSS (Inertial Navigation System / Global Navigation Satellite System) system (and maybe other sensors such as barometers and radio-altimeter). This system highly depends on the availability of GNSS signal because of the high drifts of MEMS (Microelectromechanical) inertial sensors that are used by most RPAS. Hence, if the GNSS signal becomes unavailable, the position and velocity information are lost and the RPAS will not be able to follow a given path of waypoints. When this happens, the autopilot can change the mode of operation to a safety mode in which the objective is not to follow a path of waypoints but to maintain the aircraft flying in a stable manner (e.g. orbiting around in the case of a fixed-wing RPAS or hovering in the case of a helicopter). This can be achieved using the attitude information estimated from the measurements of the inertial sensors and altitude information provided by other sensors (e.g. a barometric or radio altimeter) and the indicated air speed in the case of a fixed wing RPAS. For this reason, having an accurate attitude and heading reference system independent of GNSS is critical for the safe operation of an RPAS. It is important to note that in this safety mode the autopilot cannot control the absolute position of the aircraft so the orbit or hovering position of the aircraft can drift with time.

In literature, there are not a lot of surveys comparing KF/EKF (Kalman Filter/Extended Kalman Filter)-based AHRS (Attitude and Heading Reference System) algorithms exploiting real sensor data. In [1], a survey of AHRS algorithms for spacecraft attitude estimation is provided. However, the algorithms are compared from a mathematical point of view without comparing their accuracy and efficiency using experimental data. In addition, this survey only includes different architectures of EKF and not specific algorithms. In [2], quaternion estimators for solving Wahba's problem are compared on a qualitative and quantitative basis (based on results from Monte Carlo simulations). In [3] three EKF-based AHRS algorithms for fixed-wing RPAS are compared based on simulation results of typical fixed-wing aerial maneuvers and sensor models. There are some works proposing new AHRS algorithms and comparing the attitude estimation obtained from real sensor data with a ground truth (e.g. [4]). However, there are few papers that compare several AHRS algorithms between them.

In this paper a comparison between the implementations of different KF/EKF-based algorithms is presented. To compare these algorithms, raw measurements from the IMU and magnetometer of a commercial system (Xsens MTi-G) mounted on a rigid board have been collected. The algorithms have been implemented in Simulink and simulated with the collected raw data. One of the AHRS algorithms has also been implemented on two autopilots developed by CATEC and their performances have been compared with that of the Xsens MTi-G system.

M. Cordero, F. Alarcón and A. Viguria are at the Center for Advanced Aerospace Technologies, La Rinconada (Seville, Spain) (emails: mcordero@catec.aero, falarcon@catec.aero, aviguria@catec.aero).

A. Ollero is at the University of Seville, (Sevilla, Spain) (email: aollero@us.es).

For assessing the accuracy of AHRS systems, their attitude estimations need to be compared with ground truth values. Generally, these values are collected using a much more accurate (and more expensive) AHRS system that those under test. This reference system has to be rigidly mounted on the same body that the AHRS systems under test. In this paper, a multi-camera based motion capture system from VICON Motion System Ltd has been used to obtain attitude ground truth data. The VICON system estimates the attitude of the object from the infrared radiation emitted by the cameras and reflected from passive markers attached to the object. This system can estimate the position of each marker with sub-millimetric accuracy and the attitude of the object with an accuracy of less than a tenth of a degree so it is considered to be a good system for attitude ground truth. Motion capture systems has already been used to collect ground truth data in other works [5][6].

This paper is organized as follows: in section II the AHRS platforms that have been used for the experiments are described; in section III the mathematical background for AHRS algorithms based on EKF is provided; next, in section IV the AHRS algorithms which have been analyzed in this paper are presented; section V describes the experiments that have been carried out for comparing the different AHRS algorithms and systems; in section VI the algorithms and systems are compared using the experimental data; and finally some conclusions are shown in the last section.

II. Overview of the Autopilot Systems

RPAS safety is one of the most important issues that must be guaranteed for their integration in non segregated airspace and for their general operation. RPAS onboard systems have to be designed taking this into account.

Regarding the autopilot system, hardware redundancy has to be considered. A typical approach is to replicate the hardware (see e.g. [7]) such that in the event of experiencing a failure in the active board, the backup board could take control of the aircraft.

Another approach is to have a primary board with a microprocessor and a safety board with a microcontroller that will take control of the system when a failure is experienced by the primary board or in the event of lost of GPS data. The safety board runs an AHRS algorithm and no positioning information is estimated (only some altitude information from a barometer or other altitude sensor). With this information the safety board controls the RPAS to fly in a stable and safe way. This is the approach followed by CATEC for the development of its autopilots.

Using a feature rich microprocessor for the main board, the autopilot algorithms can be developed following a model-based design (MBD) approach [8]. However, the booting process of the operating system is slower in a microprocessor than in a microcontroller so a microcontroller is considered to be more suitable for the safety board. Following a model-based design to target a microcontroller is still possible but much more efficient algorithms are needed as these devices usually run at much lower clocks speeds and have less powerful ALUs (Arithmetic Logic Units) and FPUs (Floating Point Units). Because of this, it is important to assess the computational load of the different AHRS algorithms in addition to their accuracy.

CATEC has developed two different operational versions of its autopilot which use different inertial and magnetic sensors. Version 5 integrates a 600 $ chipset from Analog Devices (ADIS16407) with an IMU, a magnetometer and a barometer while version 6 is a low-cost version which integrates a 15 $ chipset from Invensense (MPU6000) with an IMU and a magnetometer. Both autopilots are based on a Beaglebone board which uses an ARM Cortex-A8 microprocessor running at 720 MHz with 256 MB of RAM and run QNX real time operating system. This microprocessor integrates a double precission floating point unit and a SIMD vector processor. The safety board uses an 80 MHz ARM Cortex M4 microcontroller (Texas Instruments TM4C123GH6PM) running FreeRTOS operating system. This microcontroller only has a single precision floating point unit. The performance of these two autopilots will be compared with those of Xsens MTi-G commercial system.

It's important to highlight that the Simulink implementations of the AHRS algorithms that have been used in these experiments are the same that are used to generate the C++ code that is compiled to generate the executable file that runs in CATEC autopilots for real operations.

III. KF/EKF for AHRS Algorithms

The attitude of an RPAS is defined as the inclination of its body-axes reference frame to the navigation reference frame which is generally defined as a NED (North East Down) Local Tangent Plane (LTP) reference frame. The attitude can be expressed in terms of a rotation matrix, a unitary quaternion or a sequence of Euler angles (roll, pitch and yaw). AHRS systems for RPAS are typically based on KF/EKF. Next sections will provide a mathematical background for EKF-based AHRS systems.

A. Kalman Filtering

Kalman filtering is an optimal method for estimating the state of systems with uncertain dynamics by means of the combination of noisy sensor measurements. Kalman filtering assumes that the system is linear and the measurements are linearly related with the state of the system so a discrete-time model can be described using (1) and (2).

$$\boldsymbol{x_k} = \boldsymbol{\phi_k}\boldsymbol{x_{k-1}} + \boldsymbol{w_k} \tag{1}$$

$$z_k = \boldsymbol{H}_{\mathrm{k}}\boldsymbol{x_k} + \boldsymbol{v}_{\mathrm{k}} \tag{2}$$

In (1) and (2), $\boldsymbol{x_k}$ is the state vector at instant k, $\boldsymbol{z_k}$ is the measurement vector at instant k, $\boldsymbol{\phi}_{\mathbf{k}}$ is the state transition matrix, $\boldsymbol{H_k}$ is the measurement sensitivity matrix and $\boldsymbol{w_k}$ and $\boldsymbol{v_k}$ are the white noise vectors of the system and the measurements respectively. The covariance matrices of these noises are denoted as $\boldsymbol{Q_d}$ and $\boldsymbol{R_d}$. The discrete-time model can be obtained from the equivalent continuous-time model given by (3) and (4).

$$\dot{\boldsymbol{x}}(t) = \boldsymbol{F}\,\boldsymbol{x}(\mathrm{t}) + \boldsymbol{w}(t) \tag{3}$$

$$\boldsymbol{z}(t) = \boldsymbol{H}\,\boldsymbol{z}(t) + \mathbf{v}(t) \tag{4}$$

The state transition matrix and the discrete-time covariance matrix $\boldsymbol{Q_d}$ can be obtained from the related dynamic matrix $\boldsymbol{F}$ as indicated in (5) and (6).

$$\boldsymbol{\phi} = \boldsymbol{I} + \boldsymbol{F}\Delta t \tag{5}$$

$$\boldsymbol{Q_d} = \tfrac{1}{2}(\boldsymbol{\phi Q} + \boldsymbol{Q^T}\boldsymbol{\phi^T})\Delta t \tag{6}$$

In (5) and (6) Δt is the sample time of the system and $\boldsymbol{Q}$ is the covariance matrix of the continuous time model.

Kalman filter estimates both the system state vector $\hat{\boldsymbol{x}}$ and also the uncertainty matrix of the estimation error $\widehat{\boldsymbol{P}}$ where this matrix is defined as $\boldsymbol{P} = \mathrm{E}\{(\hat{\boldsymbol{x}} - \boldsymbol{x})(\hat{\boldsymbol{x}} - \boldsymbol{x})^{\boldsymbol{T}}\}$. The process of Kalman filtering can be divided in two steps. In the first one the a priori estimations (i.e. before applying any information from the new measurements) of the state vector and the covariance matrix are calculated as indicated in (7) and (8).

$$\hat{\boldsymbol{x}}_{\boldsymbol{k}}(-) = \boldsymbol{\phi}_{\mathbf{k}}\hat{\boldsymbol{x}}_{\boldsymbol{k-1}}(+) \tag{7}$$

$$\widehat{\boldsymbol{P}}_{\boldsymbol{k}}(-) = \boldsymbol{\phi}_{\mathbf{k}}\widehat{\boldsymbol{P}}_{\boldsymbol{k-1}}(+)\boldsymbol{\phi}_{\mathbf{k}}^{\mathbf{T}} + \boldsymbol{Q_d} \tag{8}$$

In the second step the a posteriori estimations of the state vector and the covariance matrix are calculated applying the information of the new measurements using the Kalman matrix.

$$\boldsymbol{K_k} = \widehat{\boldsymbol{P}}_{\boldsymbol{k}}(-)\boldsymbol{H_k^T}\left(\boldsymbol{H_k}\boldsymbol{P_k}(-)\boldsymbol{H_k^T} + \boldsymbol{R_d}\right)^{-1} \tag{9}$$

$$\hat{\boldsymbol{x}}_{\boldsymbol{k}}(+) = \hat{\boldsymbol{x}}_{\boldsymbol{k}}(-) + \boldsymbol{K_k}(\boldsymbol{z_k} - \boldsymbol{H_k}\boldsymbol{x_k}(-)) \tag{10}$$

$$\widehat{\boldsymbol{P}}_{\boldsymbol{k}}(+) = \widehat{\boldsymbol{P}}_{\boldsymbol{k}}(-) - \boldsymbol{K_k}\boldsymbol{H_k}\widehat{\boldsymbol{P}}_{\boldsymbol{k}}(-) \tag{11}$$

In (9) - (10) $\boldsymbol{K_k}$ is the Kalman gain matrix, $\boldsymbol{Q_d}$ and $\boldsymbol{R_d}$ are the covariance matrices of the system and measurement noises respectively, and $\boldsymbol{A^{-1}}$ denotes the pseudo-inverse of matrix $\boldsymbol{A}$.

As a covariance matrix, $\widehat{\boldsymbol{P}}$ has to be a symmetric positive-definite matrix. However (11) does not guarantee that the resulting matrix fulfills these conditions [9]. To overcome this, the Joseph form of the covariance matrix as given by (12) can be used [10].

$$\boldsymbol{P_k}(+) = \left(\boldsymbol{I} - \boldsymbol{K_k}\boldsymbol{H_k}\right)\boldsymbol{P_k}(-)\left(\boldsymbol{I} - \boldsymbol{K_k}\boldsymbol{H_k}\right)^{\mathbf{T}} + \boldsymbol{K_k}\boldsymbol{R_d}\boldsymbol{K_k^T} \tag{12}$$

Kalman filtering can be extended to deal with nonlinear systems. To do this the system model is linearized around the previous estimate state vector in each iteration. The resulting method is called Extended Kalman Filtering (EKF).

B. KF/EKF-based AHRS

AHRS algorithms use the angular rate measurements from the gyroscopes ($\boldsymbol{\omega_{ib}^b}$) to update the previous attitude estimation. To do this, most systems parameterize the attitude with unitary quaternions and use the quaternion kinematics equation given by (13) and (14).

$$\boldsymbol{q_k} = \boldsymbol{q_{k-1}} + \dot{\boldsymbol{q}}_{\boldsymbol{k}} \tag{13}$$

$$\dot{\boldsymbol{q}} = \tfrac{1}{2}\begin{bmatrix} q_0 & -q_1 & -q_2 & -q_3 \\ q_1 & q_0 & -q_3 & q_2 \\ q_2 & q_3 & q_0 & -q_1 \\ q_3 & -q_2 & q_1 & q_0 \end{bmatrix}\begin{bmatrix} 0 \\ \boldsymbol{\omega_{nb}^b} \end{bmatrix} \tag{14}$$

In (14), q_0 and $[q_1 \quad q_2 \quad q_3]$ are the scalar and vector part of the quaternion respectively, $\dot{\boldsymbol{q}}$ is the derivative of $\boldsymbol{q}$ and $\boldsymbol{\omega_{nb}^b}$ is the angular rate from the body frame to the navigation frame expressed in the body frame which can be obtained from the gyroscope measurements as

$$\boldsymbol{\omega_{nb}^b} = \boldsymbol{\omega_{ib}^b} - \boldsymbol{\omega_{in}^b} \approx \boldsymbol{\omega_{ib}^b} - \boldsymbol{R_n^b}\Omega_{\mathrm{e}}\begin{bmatrix} cos(\lambda) \\ 0 \\ sin(\lambda) \end{bmatrix}. \tag{15}$$

In (15), $\boldsymbol{R_n^b}$ is the rotation matrix from the navigation frame to the body frame obtained from the previous attitude estimation, λ is the latitude of the site and Ω_{e} is the Earth rotation rate. In this equation the angular rate $\boldsymbol{\omega_{in}^b}$ has been approximated by $\boldsymbol{\omega_{ie}^b}$ which is a valid assumption for short and medium range RPAS.

After updating the previous attitude solution with the gyroscope measurements, the resulting estimation has to be corrected using a KF or EKF. The goal of this Kalman Filtering is to estimate the attitude errors in the current attitude estimation to remove them. For this purpose the attitude error is used as the state vector. This state vector can be augmented by the gyroscopes biases so they can also be compensated. However this strategy has not been followed in this work for reducing the computational load of the algorithms. AHRS algorithms that do not estimate the gyro biases are called gyro-free algorithms [11].

Kalman Filtering is implemented using the equations (7)-(11). The state transition and measurement matrices to be used depend on the specific AHRS algorithms and will be analyzed in next section. Once the attitude error is estimated, the attitude solution is corrected to remove the error. After this, the attitude error can be assumed to be zero so the state vector is set to zero. Taking this into account, the Kalman filter equations can be simplified yielding (16)-(19).

$$\widehat{\boldsymbol{P}}_{\boldsymbol{k}}(-) = \boldsymbol{\phi}_{\mathbf{k}}\widehat{\boldsymbol{P}}_{\boldsymbol{k-1}}(+)\boldsymbol{\phi}_{\mathbf{k}}^{\mathbf{T}} + \boldsymbol{Q} \tag{16}$$

$$\boldsymbol{K_k} = \widehat{\boldsymbol{P}}_{\boldsymbol{k}}(-)\boldsymbol{H_k^T}\left(\boldsymbol{H_k}\boldsymbol{P_k}(-)\boldsymbol{H_k^T} + \boldsymbol{R}\right)^{-1} \tag{17}$$

$$\hat{\boldsymbol{x}}_{\boldsymbol{k}}(+) = \boldsymbol{K_k}\boldsymbol{z_k} \tag{18}$$

$$\boldsymbol{P_k}(+) = (\boldsymbol{I} - \boldsymbol{K_k}\boldsymbol{H_k})\boldsymbol{P_k}(-)(\boldsymbol{I} - \boldsymbol{K_k}\boldsymbol{H_k})^{\mathbf{T}} + \boldsymbol{K_k}\boldsymbol{R}\boldsymbol{K_k^T} \tag{19}$$

The measurements of the attitude errors of the current attitude estimation are obtained using the measurements provided by the auxiliary sensors (i.e. the accelerometers and the magnetometer). The magnetometer measurements are used to calculate the yaw of the RPAS and the difference between this value and the current estimation is used as the measurement of the yaw error. In a similar way, the outputs of the accelerometers are used to calculate the measurements of the roll and pitch errors. To do this, the RPAS has to be in a non accelerated state in which the gravity is the only acceleration that is measured by the accelerometers. When this condition is fulfilled, the measured acceleration in the body frame can be compared with the gravity acceleration in the navigation frame and roll and pitch angles can be calculated. More details on this will be given in next section.

To sum up, the measurement cycle is always running for the yaw error component (obtained from the magnetometer) and it's only run for the roll and pitch error components when

the measured acceleration in the navigation frame is close enough to the gravity.

IV. Attitude and Heading Reference Systems

In this section the three different KF/EKF-based AHRS systems that are compared in this paper are presented.

A. Setoodeh's AHRS algorithm.

The estimated rotation matrix from the navigation to the body frame ($\boldsymbol{R}_{\boldsymbol{n}}^{\boldsymbol{b}_{est}}$) can be related with the actual rotation matrix ($\boldsymbol{R}_{\boldsymbol{n}}^{\boldsymbol{b}}$) as $\boldsymbol{R}_{\boldsymbol{n}}^{\boldsymbol{b}} = \boldsymbol{R}_{\boldsymbol{b}_{est}}^{\boldsymbol{b}} \boldsymbol{R}_{\boldsymbol{n}}^{\boldsymbol{b}_{est}} = (\boldsymbol{I} - skew(\boldsymbol{\varepsilon}))\boldsymbol{R}_{\boldsymbol{n}}^{\boldsymbol{b}_{est}}$ where $\boldsymbol{\varepsilon} = [\delta\phi \quad \delta\theta \quad \delta\psi]^{\mathrm{T}}$ are the Euler angular errors obtained from the matrix $\boldsymbol{R}_{\boldsymbol{b}_{est}}^{\boldsymbol{b}}$. In the algorithm proposed by Setoodeh et al [12] these angular errors are used as the state vector for the Kalman Filter so the state vector can be expressed as $\boldsymbol{x} = \boldsymbol{\varepsilon}$.

This is an EKF-based algorithm because the dynamic matrix of the Euler angular errors has to be obtained from the linearization of the kinematic equations of the Euler angles which are given by

$$\begin{bmatrix} \dot{\phi} \\ \dot{\theta} \\ \dot{\psi} \end{bmatrix} = \begin{bmatrix} 1 & sen(\phi)tan(\theta) & cos(\phi)tan(\theta) \\ 0 & cos(\phi) & -sen(\phi) \\ 0 & sen(\phi)/cos(\theta) & cos(\phi)/cos(\theta) \end{bmatrix} \boldsymbol{\omega}_{\mathbf{bn}}^{\mathbf{b}}. \tag{20}$$

When these equations are linearized with respect to the Euler angles the resulting dynamic matrix of the system is

$$\boldsymbol{F} = \begin{bmatrix} t\theta(c\phi\omega_y - s\phi\omega_z) & (1+(t\theta)^2)(s\phi\omega_y + c\phi\omega_z) & 0 \\ -(s\phi\omega_y + c\phi\omega_z) & 0 & 0 \\ (c\phi\omega_y - s\phi\omega_z)/c\theta & t\theta(s\phi\omega_y + c\phi\omega_z)/c\theta & 0 \end{bmatrix}. \tag{21}$$

In (21) $s\theta$, $c\theta$ and $t\theta$ denote the sine, cosine and tangent of the angle θ respectively while ω_x, ω_y and ω_z are the components of $\boldsymbol{\omega}_{\mathbf{bn}}^{\mathbf{b}}$.

The measurement vector contains the differences between the current estimated attitude angles and the attitude angles calculated from the measurements of the magnetometer and accelerometers calculated from (23)-(25). The measurement vector can then be expressed as

$$\boldsymbol{z} = \boldsymbol{\varepsilon} = [\phi_m - \hat{\phi} \quad \theta_m - \hat{\theta} \quad \psi_m - \hat{\psi}]. \tag{22}$$

The measurement matrix is the identity matrix (i.e. $\boldsymbol{H} = \boldsymbol{I}$). ϕ_m, θ_m and ψ_m are the attitude angles calculated from the sensor measurements while $\hat{\phi}$, $\hat{\theta}$ and $\hat{\psi}$ are the current estimations of the Euler angles. When the measured acceleration deviates from the gravity more than a certain threshold, the measurement vector is given by $\boldsymbol{z} = [0 \quad 0 \quad \psi_m - \hat{\psi}]$ so only the estimation of the heading is corrected. The roll and pitch angles are calculated from the measurements of the accelerometers as indicated in (23) and (24).

$$\phi_m = arctan(a_y^b / a_z^b) \tag{23}$$

$$\theta_m = arctan(a_x^b / \sqrt{(a_y^b)^2 + (a_z^b)^2}) \tag{24}$$

In (23) and (24) a_x, a_y and a_z are the components of the measurements of the accelerometers in the body frame. The yaw angle is calculated from the magnetometer measurements as

$$\psi_m = -atan\left(\frac{c\phi m_y^b - s\phi m_z^b}{c\theta m_x^b + s\theta s\phi m_y^b + s\theta c\phi m_z^b}\right) + D \tag{25}$$

In (25), m_x, m_y and m_z are the components of the magnetometer measurements in the body frame, and D is the magnetic declination angle.

When the a posteriori attitude error estimation is obtained from (18), this error can be removed from the current attitude estimation using the following equation [13]

$$\boldsymbol{R}_{\boldsymbol{n}}^{\boldsymbol{b}}(+) = (\boldsymbol{I} - skew(\hat{\boldsymbol{x}}(+)))\boldsymbol{R}_{\boldsymbol{n}}^{\boldsymbol{b}}(-) \tag{26}$$

In (26), $\boldsymbol{R}_{\boldsymbol{n}}^{\boldsymbol{b}}(-)$ and $\boldsymbol{R}_{\boldsymbol{n}}^{\boldsymbol{b}}(+)$ are the rotation matrices corresponding to the current attitude estimation before and after the correction respectively, and $skew(\boldsymbol{v})$ denotes the skew-symmetric matrix of vector $\boldsymbol{v}$ which is given by

$$skew(\mathbf{v}) = \begin{bmatrix} 0 & -v_3 & v_2 \\ v_3 & 0 & -v_1 \\ -v_2 & v_1 & 0 \end{bmatrix} \tag{27}$$

B. Han's AHRS algorithm

The estimated rotation matrix from the body to the navigation frame ($\boldsymbol{R}_{\boldsymbol{b}}^{\boldsymbol{n}_{est}}$) can be related with the actual rotation matrix ($\boldsymbol{R}_{\boldsymbol{b}}^{\boldsymbol{n}}$) as $\boldsymbol{R}_{\boldsymbol{b}}^{\boldsymbol{n}} = \boldsymbol{R}_{\boldsymbol{n}_{est}}^{\boldsymbol{n}} \boldsymbol{R}_{\boldsymbol{b}}^{\boldsymbol{n}_{est}} = (\boldsymbol{I} - skew(\boldsymbol{\varphi}))\boldsymbol{R}_{\boldsymbol{b}}^{\boldsymbol{n}_{est}}$ where $\boldsymbol{\varphi} = [\varphi_N \quad \varphi_E \quad \varphi_D]^{\mathrm{T}}$ are the angular errors obtained from the matrix $\boldsymbol{R}_{\boldsymbol{n}_{est}}^{\boldsymbol{n}}$. In the algorithm proposed by Han et al [14], these angular errors are used as the state vector for the Kalman Filter so the state vector can be expressed as $\boldsymbol{x} = \boldsymbol{\varphi}$.

The dynamic matrix is given by $\boldsymbol{F} = -skew(\boldsymbol{\omega}_{\mathbf{in}}^{\mathbf{n}})$ where $\boldsymbol{\omega}_{\mathbf{in}}^{\mathbf{n}}$ is calculated as

$$\boldsymbol{\omega}_{\mathbf{in}}^{\mathbf{n}} = \boldsymbol{\omega}_{\mathbf{ie}}^{\mathbf{n}} + \boldsymbol{\omega}_{\mathbf{en}}^{\mathbf{n}} \approx \Omega_e \begin{bmatrix} cos(\lambda) \\ 0 \\ sin(\lambda) \end{bmatrix}. \tag{28}$$

In (28), $\boldsymbol{\omega}_{\mathbf{en}}^{\mathbf{n}}$ has been neglected as it was done in (15), which is a valid assumption for short and medium range RPAS. For the purpose of attitude estimation of short range RPAS, fixed latitude λ can be considered. Under this assumption $\boldsymbol{F}$ is a constant matrix and it doesn't need to be recalculated at each iteration and no trigonometric operations are involved. In addition, no linearization process has been performed to get this matrix. This differs from Setoodeh's algorithm in which a state transition matrix that needs to be recalculated at each iteration involving trigonometric operations.

The measurement vector is built in the same way as in Setoodeh's algorithm so it can be expressed as in (22). However, in this case these Euler angle errors which are expressed in the body frame need to be related to the Euler angle errors expressed in the navigation frame which are used as the state vector. To get this matrix the equations that relate these two sets of angles need to be established. For the sake of brevity, the process of deriving the measurement matrix is not being shown in this paper and this matrix is directly presented as

$$\boldsymbol{H} = \begin{bmatrix} -cos(\psi)/cos(\theta) & -sen(\psi)/cos(\theta) & 0 \\ sen(\psi) & -cos(\psi) & 0 \\ -tan(\theta)cos(\psi) & -tan(\theta)sen(\psi) & -1 \end{bmatrix}. \quad (29)$$

This measurement matrix is more complex than the one of Setoodeh's algorithm. As in Setoodeh's algorithm, when the measured acceleration deviates from the gravity more than a certain threshold only the estimation of the heading is corrected.

Finally, when the a posteriori attitude error estimation is calculated, this error can be removed from the current attitude estimation using the equation

$$\boldsymbol{R}_b^n(+) = (\boldsymbol{I} - skew(\hat{\boldsymbol{x}}(+)))\boldsymbol{R}_b^n(-). \quad (30)$$

C. Wang's AHRS algorithm

In this algorithm proposed by Wang et al [15][16] the angular errors obtained from the matrix $\boldsymbol{R}_{n_{est}}^{n}$ are used as the state vector for a Kalman Filter as in Han's algorithm. The dynamic matrix is then calculated as $\boldsymbol{F} = -skew(\boldsymbol{\omega}_{in}^{n})$ which is the same dynamic matrix than that of Han's algorithm.

Wang's algorithm differs from Han's algorithm in the measurement model. In this case, the raw measurements of the accelerometers in the body axes are compared to the expected acceleration in the navigation frame when the RPAS is in non accelerated state. Under this condition, the acceleration in the navigation frame should be equal to the gravity, i.e. $\boldsymbol{a}^n = [0 \quad 0 \quad -g]^{\mathbf{T}}$ (keep in mind that a NED Local Tangent Plane frame is used as the navigation frame). The difference between the measured acceleration and the expected acceleration can be related to estimate the attitude error of the current attitude estimation as

$$\boldsymbol{\delta a}^n = \boldsymbol{a}_m^n - \boldsymbol{a}^n = (\boldsymbol{I} - skew(\boldsymbol{\varphi}))\boldsymbol{R}_b^n \, \boldsymbol{a}^b - \boldsymbol{R}_b^n \boldsymbol{a}^b. \quad (31)$$

Making some simple operations (28) can be rewritten as

$$\boldsymbol{\delta a}^n = -skew(\boldsymbol{\varphi})\boldsymbol{a}^n = skew(\boldsymbol{a}^n)\boldsymbol{\varphi} = \begin{bmatrix} 0 & -g & 0 \\ g & 0 & 0 \\ 0 & 0 & 0 \end{bmatrix} \boldsymbol{\varphi}. \quad (32)$$

The third component of $\boldsymbol{\delta a}^n$ does not provide any information for estimating $\boldsymbol{\varphi}$ as can be deduced from (29). In addition, it can be noted that the third component of $\boldsymbol{\varphi}$ cannot be estimated using the information in $\boldsymbol{\delta a}^n$. This vector is calculated as

$$\delta \boldsymbol{a}^n = \boldsymbol{R}_b^n \boldsymbol{a}_m^b - \begin{bmatrix} 0 \\ 0 \\ -g \end{bmatrix}. \quad (33)$$

To estimate the third component of $\boldsymbol{\varphi}$ the heading error $\delta\psi = \psi_m - \hat{\psi}$ obtained from the magnetometer measurements is used. Then, the measurement vector and the measurement matrix can be expressed as

$$\boldsymbol{z} = [\delta a_1^n \quad \delta a_2^n \quad \psi_m - \hat{\psi}] \quad (34)$$

$$\boldsymbol{H} = \begin{bmatrix} 0 & -g & 0 \\ g & 0 & 0 \\ 0 & 0 & -1 \end{bmatrix} \quad (35)$$

As in the previous algorithms, when the measured acceleration deviates from the gravity more than a certain threshold only the estimation of the heading is corrected.

The attitude estimation is corrected with the estimated attitude error applying (26). Note that in this algorithm both the dynamic and the measurement matrices are constants for short range RPAS so the computational load is expected to be lower than that of Seetodeh's and Han's algorithms. This will be confirmed by the results of the experiments shown in section VI.

A drawback of Wang's algorithm is that the measurement model directly uses the difference between the gravity field in the navigation frame and the measurements of the accelerometers in the body frame. The gravity field in the navigation frame is supposed to be known and constant (usually 9.81 m/s^2 is used). However, the gravity field slightly varies with the latitude and the altitude of the platform. These variations can cause additional errors in the attitude estimations. In Setoodeh's and Han's algorithms this is not a problem since their measurement models use the differences between the current estimation of roll and pitch and the estimation obtained with the accelerometer measurements.

V. Experiments

The implementations of the AHRS algorithms under test have been compared from two different points of view: accuracy and efficiency. For this purpose two types of experiments have been carried out. These experiments will be described in the next sections. Additionally, the performance of one of the AHRS implementations running on the two versions of CATEC's autopilot has been compared with the Xsens MTi-G commercial AHRS systems.

Each type of experiment has been performed ten times under different conditions (i.e. different angular speeds and accelerations) and a data set has been logged in each of them. The performance results presented in this paper (TABLE I. to TABLE VII.) have been obtained as an average of all the data sets collected during the experiments.

A. Experiments for testing accuracy

CATEC has an indoor multi-vehicle aerial testbed that can be used to develop and test different algorithms applied to multiple aerial platforms. The tests can be conducted in a 15 m x 15 m x 5 m volume. The testbed has an indoor localization system based on 20 VICON cameras (see Fig. 1) that can provide the position and attitude of an object with high accuracy (sub-millimetric accuracy for position and better than a tenth of a degree for attitude). To estimate the position and attitude of an object, the system only needs that passive markers are attached to it. The basic operation of the system is as follows: the cameras emit infra-red radiation that are reflected by the passive markers; then the reflected radiation are received by the cameras and they estimate the time of flight of the light wave; with the information of all the cameras the system finally estimates the position and

attitude of the object. The sample rate of data acquisition can be configured by the user up to 500 Hz although in these experiments 200 Hz were used.

To perform this test, the three systems under test (the two versions of CATEC's autopilot and the Xsens MTi-G) have been mounted on a rigid board to which VICON markers have been attached as shown in Fig. 2. During the experiment the board has been moved by hand so its attitude has been continuously changed for about ten minutes. This experiment has been repeated ten times and the raw measurements from the inertial and magnetic sensors of the three systems and the attitude estimations provided by the Xsens MTi-G have been logged during those periods together with the attitude estimation provided by the VICON system. During each of these times different attitude rates and different accelerations have been applied to the board. The collected data have been synchronized using a common VICON signal to avoid time lags between logs.

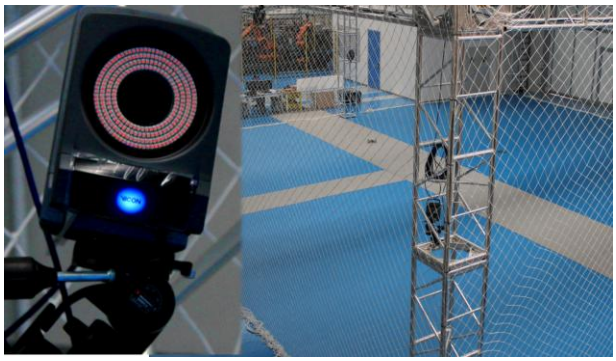

Figure 1. VICON camera (left) and CATEC indoor test bed (right)

To compare the implementations of the AHRS algorithms, the Xsens MTi-G raw measurements have been fed into the Simulink implementations of the AHRSs algorithms to get the attitude estimations. These attitude estimations have been compared with the attitude provided by the Xsens MTi-G and the attitude provided by the VICON system. Although the AHRS systems have been tried to be mounted perfectly aligned on the board and also the initial attitude of the board has been tried to be aligned with VICON reference system, misalignments are unavoidable. In addition, VICON reference system can be also misaligned with the local tangent plane reference frame used as the navigation frame by Xsens MTi-G and CATEC autopilots. To mitigate the effects of these misalignments, all the attitude estimations have been post-processed so the initial attitude estimations match for all the algorithms. The residual misalignments can be neglected and hence they do not have any effect on the AHRS comparison results. Section VI presents the comparison of the attitude estimations.

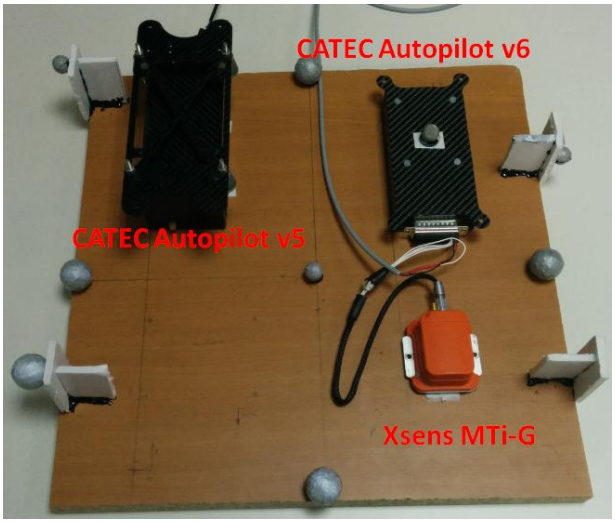

Figure 2. AHRS systems rigidly mounted on the test board with VICON markers

B. *Experiment for testing efficiency*

To perform this test, the three AHRS algorithms have been run in an ARM Cortex M4 microcontroller integrated in the safety board of CATEC's autopilot. In order to do this, C++ code has been generated from each AHRS Simulink model using the code generation tool from The MathWorks. This code has been compiled for the ARM Cortex M4 using the Code Composer Studio IDE from Texas Instruments. The algorithms have been run while the board remained static so attitude corrections using the measurements of the accelerometers have been done in each iteration of the algorithm (because RPAS is in non accelerated state). To compare the AHRS algorithms the CPU load and used RAM memory have been checked. In addition the minimum possible step time has been measured.

VI. COMPARISON OF AHRS

In this section the results of the experiments are provided. The observed performances of the different systems during the whole set of experiments have been expressed in terms of the estimation accuracy and the algorithm efficiency. These two parameters have been quantified and their values have been gathered in several tables. Some figures showing the attitude estimations provided by the different algorithms in some time slots of the experiments.

A. *Accuracy of AHRS algorithms*

In this section, the accuracy of the three tested AHRS algorithms and the AHRS algorithm of the Xsens MTi-G system are compared using the attitude estimation of the VICON system as the true reference. For this comparison the raw measurements of Xsens MTi-G inertial and magnetic sensors have been fed into the Simulink implementations so all the algorithms are run using the same sensors.

It can be seen from TABLE I. to TABLE III. that the algorithms by Han and Wang provide better accuracies when estimating the roll and yaw angles and the accuracies obtained with Setoodeh's algorithm and the one used by the Xsens MTi-G system are slightly worse. In addition, Han's algorithm provides the better accuracy when estimating the

heading in comparison with the other three algorithms. Hence, Han's algorithm provides the best overall accuracy and it has been chosen to be implemented in CATEC's autopilot.

Fig. 3 to Fig. 5 show the attitude estimations obtained for the different algorithms in particular time slots of one of the experiments particular experiment. They are only intended to provide visual information of the AHRS outputs.

TABLE I. ROLL ACCURACY OF AHRS ALGORITHMS

AHRS	Roll accuracy of AHRS Algorithms	
	Mean error (RMS) [deg]	*Standard deviation [deg]*
Han	0.43	0.63
Setoodeh	0.50	0.72
Wang	0.43	0.63
Xsens MTi-G	0.54	0.67

TABLE II. PITCH ACCURACY OF AHRS ALGORITHMS

AHRS	Pitch accuracy of AHRS Algorithms	
	Mean error (RMS) [deg]	*Standard deviation [deg]*
Han	0.53	0.65
Setoodeh	0.71	0.82
Wang	0.57	0.67
Xsens MTi-G	0.78	0.61

TABLE III. YAW ACCURACY OF AHRS ALGORITHMS

AHRS	Yaw accuracy of AHRS Algorithms	
	Mean error (RMS) [deg]	*Standard deviation [deg]*
Han	1.37	0.97
Setoodeh	1.76	1.20
Wang	1.78	1.15
Xsens MTi-G	3.09	1.48

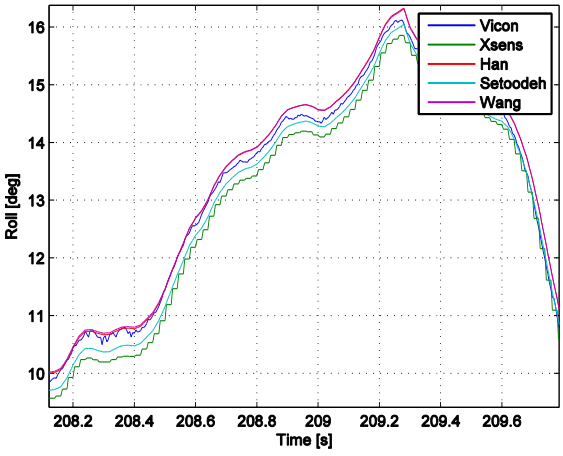

Figure 3. Roll estimations obtained with the different algorithms

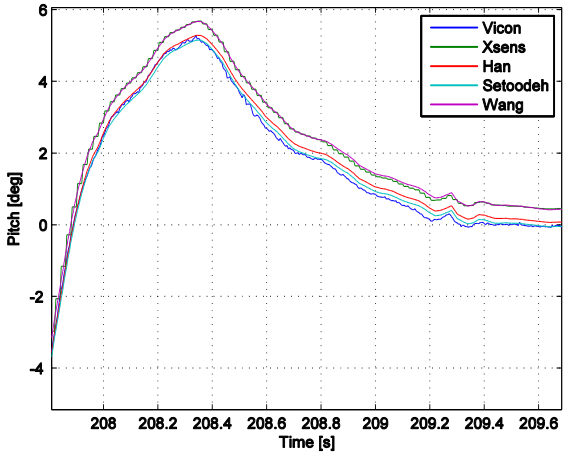

Figure 4. Pitch estimations obtained with the different algorithms

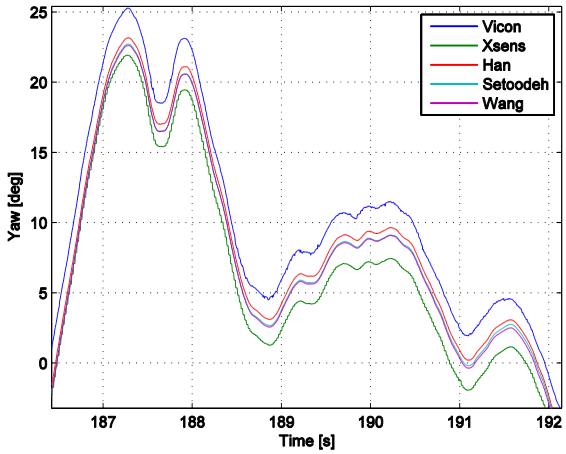

Figure 5. Yaw estimations obtained with the different algorithms

B. *Accuracy of AHRS systems*

In this section, the accuracies of CATEC AHRS systems are compared with that provided by the Xsens MTi-G system. Remind from section II**¡Error! No se encuentra el origen de la referencia.** that version 5 of CATEC autopilot integrates a 600 $ sensors' chipset from Analog Devices (ADIS16407) while version 6 integrates a 15 $ chipset from Invensense (MPU6000).

The results have been gathered in TABLE IV. to TABLE VI. . The results show that the accuracies of roll estimations of CATEC v5 autopilot and Xsens MTi-G system are quite similar and are better than that of CATEC v6 autopilot. With respect to the pitch estimations, both CATEC v5 and CATEC v6 autopilots provide similar accuracies that are better than that provided by Xsens MTi-G system. Finally, yaw estimations provided by CATEC v5 autopilot are more accurate than those provided by CATEC v6 and quite more accurate than those provided by Xsens MTi-G system. CATEC v5 has proved to be the more accurate system of the three. However, it's important to note that CATEC v6 also provides good attitude estimations despite using much cheaper sensors. Because of this reason, it can be used by low cost budget-constraint systems.

TABLE IV. ROLL ACCURACY OF AHRS SYSTEMS

AHRS	Roll accuracy of AHRS Systems	
	Mean error (RMS) [deg]	*Standard deviation [deg]*
CATECv5	0.59	0.78
CATECv6	0.76	1.13
Xsens MTi-G	0.54	0.67

TABLE V. PITCH ACCURACY OF AHRS SYSTEMS

AHRS	Pitch accuracy of AHRS Systems	
	Mean error (RMS) [deg]	*Standard deviation [deg]*
CATECv5	0.47	0.60
CATECv6	0.43	0.59
Xsens MTi-G	0.78	0.61

TABLE VI. YAW ACCURACY OF AHRS SYSTEMS

AHRS	Yaw accuracy of AHRS Systems	
	Mean error (RMS) [deg]	*Standard deviation [deg]*
CATECv5	0.81	0.97
CATECv6	1.25	1.04
Xsens MTi-G	3.09	1.48

Fig. 6 to Fig. 8 show the attitude estimations obtained for the different AHRS systems in particular time slots of one of the experiments particular experiment. They are only intended to provide visual information of the outputs of the AHRS systems.

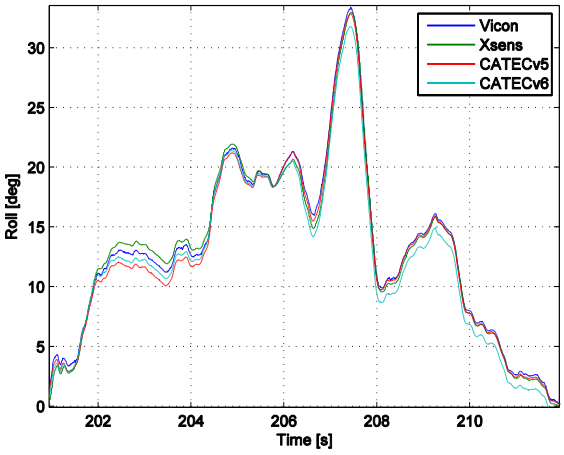

Figure 6. Roll estimations obtained with the different systems

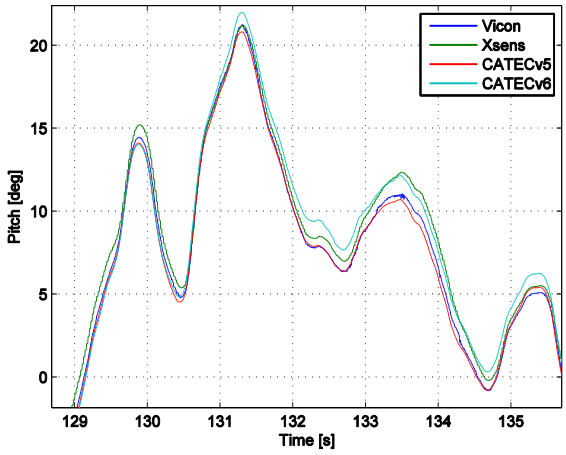

Figure 7. Pitch estimations obtained with the different systems

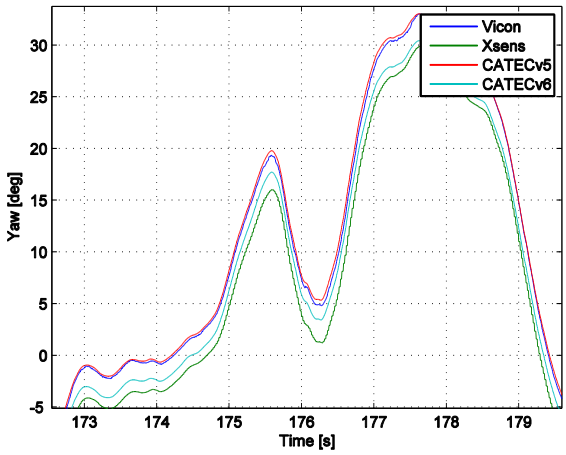

Figure 8. Yaw estimations obtained with the different systems

C. *Efficiency*

The results of the efficiency experiments are shown in TABLE VII. Wang algorithm presents the best performance in terms of CPU load and minimum step time. This was expected since it uses the simplest state transition and measurement matrices of the three algorithms. From TABLE VII it can be seen that there is not a significant difference between Han's and Setoodeh's algorithms with respect to the CPU load and minimum step time. The CPU load and minimum step time are practically the same for Setoodeh's and Han's algorithms. This could be also expected because, although the state transition matrix of Seetodeh's is more complex than that of Han's algorithm and it has to be updated in each iteration, the measurement matrix of Han's algorithm is more complex than that of Setoodeh's algorithm. The final result is that both have similar computational loads. Finally, it can be seen that all tested AHRS algorithms use the same amount of RAM memory.

TABLE VII. AHRS EFFICIENCY PARAMETERS

AHRS	Efficiency Parameters

	CPU load	*Minimum Step Time*	*RAM*
Han	~8%	~0.38 ms	~1.5 KB
Setoodeh	~8%	~0.38 ms	~1.5 KB
Wang	~3%	~0.11 ms	~1.5 KB

VII. CONCLUSION

In this paper, three different EKF-based AHRS algorithms have been compared. For the comparison, the algorithms have been implemented in Simulink and attitude estimations provided by a VICON indoor positioning system have been used as the true reference. In addition, the computational load and memory requirements of the three algorithms have been evaluated. Wang's algorithm has been proved to be the most efficient one of the three, but Han's algorithm has been shown to provide the best overall accuracy (particularly in heading estimation). In addition, Han's algorithm provides better accuracy than the algorithm used by Xsens MTi-G system so it has been chosen for CATEC AHRS system.

Han's algorithm has been implemented in two autopilots developed by CATEC which use sets of sensors of different costs (version 6 uses cheaper sensors than version 5). The accuracies of the attitude estimations provided by these two autopilots have been compared with the accuracy of the Xsens MTi-G. According to the experiment's results, the accuracy of attitude estimations provided by CATEC v5 autopilot is better than that of the attitude estimations provided by CATEC v6 and the Xsens MTi-G systems. CATEC v6 can be used for low cost systems because it provides acceptable accuracies using much cheaper sensors than CATEC v6 autopilot and it is much cheaper than Xsens MTi-G.

REFERENCES

[1] J. L. Crassidis, F. L. Markley, and Y. Cheng, "Survey of Nonlinear Attitude Estimation Methods," *J. Guid. Control. Dyn.*, vol. 30, no. 1, pp. 12–28, Jan. 2007.

[2] D. Choukroun, "Novel Methods for Attitude Determination Using Vector Observations," Israel Institute of Technology, 2003.

[3] R. R. Lima and L. a. B. Torres, "Performance Evaluation of Attitude Estimation Algorithms in the Design of an AHRS for Fixed Wing UAVs," in *2012 Brazilian Robotics Symposium and Latin American Robotics Symposium*, 2012, no. 2, pp. 255–260.

[4] G. Sun, M. Garratt, and C. Wang, "Implementing quaternion based AHRS on a MEMS multisensor hardware platform," in *International Global Navigation Satellite Systems Society IGNSS Symposium 2013*, 2013.

[5] J. Macdonald, R. Leishman, R. Beard, and T. McLain, "Analysis of an Improved IMU-Based Observer for Multirotor Helicopters," *J. Intell. Robot. Syst.*, pp. 1–21, May 2013.

[6] A. Bry, A. Bachrach, and N. Roy, "State estimation for aggressive flight in GPS-denied environments using onboard sensing," *2012 IEEE Int. Conf. Robot. Autom.*, no. Icra, pp. 1–8, May 2012.

[7] Sarah Vellely, "MP2128-3x MicroPilot's Triple Redundant UAV Autopilot," 2010.

[8] D. Santamaría, F. Alarcón, A. Jiménez, A. Viguria, M. Béjar, and A. Ollero, "Model-Based Design, Development and Validation for UAS Critical Software," *J. Intell. Robot. Syst.*, vol. 65, no. 1–4, pp. 103–114, Aug. 2011.

[9] A. Schumacher, "Integration of a GPS aided Strapdown Inertial Navigation System for Land Vehicles," KTH, 2006.

[10] M. S. Grewal and A. P. Andrews, *Kalman Filtering Theory and Practice Using MATLAB*, 3rd ed. John Wiley & Sons, Inc., 2008.

[11] D. Gebre-Egziabher and G. H. Elkaim, "MAV attitude determination by vector matching," *IEEE Trans. Aerosp. Electron. Syst.*, vol. 44, no. 3, pp. 1012–1028, Jul. 2008.

[12] P. Setoodeh, A. Khayatian, and E. Frajah, "Attitude Estimation By Separate-Bias Kalman Filter-Based Data Fusion," *J. Navig.*, vol. 57, no. 2, pp. 261–273, May 2004.

[13] E. Bekir, *Introduction to Modern Navigation Systems*. 2007.

[14] S. Han and J. Wang, "A Novel Method to Integrate IMU and Magnetometers in Attitude and Heading Reference Systems," *J. Navig.*, vol. 64, no. 04, pp. 727–738, Sep. 2011.

[15] M. Wang, R. R. Hatch, and Y. Yang, "Adaptive filter for a miniature MEMS based attitude and heading reference system," in *PLANS 2004. Position Location and Navigation Symposium (IEEE Cat. No.04CH37556)*, 2004, pp. 193–200.

[16] W. Li and J. Wang, "Effective Adaptive Kalman Filter for MEMS-IMU/Magnetometers Integrated Attitude and Heading Reference Systems," *J. Navig.*, vol. 66, no. 01, pp. 99–113, Jul. 2012.